



## Room-temperature electrosynthesized ZnO thin film with strong (0 0 2) orientation and its optical properties

Y.F. Mei<sup>a,\*</sup>, G.G. Siu<sup>a</sup>, Ricky K.Y. Fu<sup>a</sup>, Paul K. Chu<sup>a</sup>, Z.M. Li<sup>b</sup>, Z.K. Tang<sup>b</sup>

<sup>a</sup> Department of Physics and Materials Science, City University of Hong Kong, Kowloon, Hong Kong, China

<sup>b</sup> Department of Physics, Hong Kong University of Science & Technology, Clear Water Bay, Kowloon, Hong Kong, China

Received 17 January 2005; received in revised form 3 May 2005; accepted 3 May 2005

Available online 23 June 2005

### Abstract

ZnO thin film with strong orientation (0 0 2) and smooth surface morphology was electrosynthesized on ITO-coated glass substrate at room temperature under pulsed voltage. Photoluminescence (PL) shows two obvious peaks: violet band and strong green band. The former is due to the free-excitonic transition and the latter is believed to arise from the single ionized oxygen vacancy ( $V_O^+$ ). Raman scattering reveals that the  $580\text{ cm}^{-1}$  mode and the shoulder peak mode at  $550\text{ cm}^{-1}$  originate from the N-related local vibration mode (LVM) and  $E_1$  (LO) mode, respectively.

© 2005 Elsevier B.V. All rights reserved.

PACS: 71.55.Gs; 81.15.Pq; 78.55.-m; 78.30.-j

Keywords: II-VI semiconductors; Electrodeposition; Photoluminescence; Infrared and Raman spectra

### 1. Introduction

Zinc oxide (ZnO) films, which possess many interesting properties such as piezoelectric effect, conductive effects, acoustic characteristics, direct band gap (3.3 eV), and absence of toxicity, have recently attracted much attention, because of their potential applications in optoelectronic devices such as solar cells and displays [1–4]. Different methods

have been employed to prepare ZnO films including chemical vapor deposition (CVD), thermal oxidation, radio frequency magnetron sputtering, pulsed laser deposition, electron beam evaporation, spray pyrolysis, and electrodeposition [5–11]. Among them, electrodeposition from aqueous solutions is a simple, environmentally friendly, and low-cost technique, by which uniform films with controlled stoichiometry can be produced [12].

This paper reports the preparation and characterization of ZnO thin films with strong orientation (0 0 2) on ITO-coated glass substrate by an electrosynthesized method at room temperature under pulsed

\* Corresponding author. Tel.: +852 21942824;

fax: +852 27887830.

E-mail address: [meiyongfeng@nju.org.cn](mailto:meiyongfeng@nju.org.cn) (Y.F. Mei).

voltage. Photoluminescence (PL) shows a salient violet band as well as a strong green band. The former is due to the free-excitonic transition and the latter appears to arise from the single ionized oxygen vacancy ( $V_{O}^+$ ) that disappears after annealing. The Raman peaks near  $580\text{ cm}^{-1}$  has two different origins.

## 2. Experiments

ZnO thin films were electrosynthesized at room temperature ( $20\text{ }^{\circ}\text{C}$ ) on ITO-coated glass substrates in an aqueous solution containing  $0.1\text{ M}$  zinc nitrate with a pH of about 5.0. Rectangular voltage pulses (pulsing period of 20 ms and pulsing width on time of 1 ms) were used in our experiment. The amplitude of the pulsed voltage was  $-1\text{ V}$ . During the electrodeposition process, a two-electrode arrangement was used in which the ITO-coated glass served as the anode and zinc sheet (99.99%) the cathode. Nitrate ions were used as the oxygen precursor. X-ray diffraction (XRD) analysis was performed with a Siemens D500 diffractometer using the  $\text{Cu K}\alpha$  line at  $1.5406\text{ \AA}$ . PL measurements were taken using a He–Cd laser light ( $325\text{ nm}$ ) at room temperature and detected by a photon counting system with a photomultiplier.

## 3. Results and discussions

Fig. 1a shows the X-ray diffraction patterns of the ZnO films deposited at room temperature ( $20\text{ }^{\circ}\text{C}$ ) for about 180 min under pulsed voltage of  $-1\text{ V}$ . The deposition rate at  $-1\text{ V}$  is about  $300\text{ nm/h}$ . The XRD spectra acquired from the as-deposited film reveals a preferential (0 0 2) orientation, i.e.  $c$ -axis orientation, along which the density of surface energy per plane is minimal. The other two weak peaks at (1 0 0) and (1 0 1) can be seen only after annealing at  $400\text{ }^{\circ}\text{C}$  for 30 min. The (0 0 2) peak intensity, that is, the preferential orientation is found to increase with higher annealing temperature. Fig. 1b shows the surface morphology of the as-deposited ZnO film on ITO-coated glass substrate by the scanning electron microscopy (SEM, JEOL JSM-6300) measurement. The surface of ZnO film synthesized at room temperature is much smoother than that at high temperature (such as  $60\text{ }^{\circ}\text{C}$ ), which generally presents

the forms of coarse crystals, such as thorny shape, fibrous sheet, and nodular appearance [11,12]. So, our method can supply a way to fabricate ZnO film with good quality.

Generally, ZnO can emit three luminescence bands in the ultraviolet (UV), green, and yellow regions [8]. In Fig. 2, the effects of thermal annealing on the PL properties of ZnO films are shown. The UV emission is due to the direct recombination of photogenerated charge carriers (exciton emission) [13]. As the annealing temperature increases, the intensity of the UV emission ( $377\text{ nm}$ ) goes up as shown in Fig. 2(left). Furthermore, a red-shift behavior from  $377$  to  $394\text{ nm}$  with increasing the annealing temperature manifests. Similar result have been reported for ZnO films deposited onto InP substrate [14]. Tang et al. reported that UV PL was related to the microstructure of small ZnO crystalline [13]. Our XRD pattern shows the degradation of the crystal structure in the ZnO film after annealing; thereby suggesting that it may be the cause of the changes in the intensity and peak position of the UV band ( $377\text{ nm}$ ). However, it has recently been reported that the intensity of the UV emission peak exhibits no clear dependence on the crystal quality, and so the detailed explanation needs additional PL investigation at low temperature [15].

In addition to the UV band ( $377\text{--}395\text{ nm}$ ), there are several visible emission bands ( $430, 530, 570,$  and  $666\text{ nm}$ ) originating from our ZnO films. Some researchers have reported that the visible emission of the ZnO film is related to different intrinsic defects such as oxygen vacancies, zinc vacancies, zinc interstitials, oxygen interstitials, and antisite defect [8,16–18]. However, due to the complexity of the microscopic details, the exact origin of the visible emission in ZnO is not yet well understood [8]. Strong green emission ( $570\text{ nm}$ ) was observed from our as-deposited ZnO film and it has been reported by Vanheusden et al. to come from oxygen vacancies [ $V_{O}^+$ ] [16]. Wu et al. reported that the strong green emission in oxygen-deficient ZnO films was severely influenced by the oxygen pressure and growth temperature [8]. Usually, a high temperature such as  $65\text{ }^{\circ}\text{C}$  is adopted in the electrodeposition of ZnO film, but in our experiments, room temperature was used to mitigate oxidation during growth. The disappearance of the strong green emission ( $570\text{ nm}$ ) after annealing

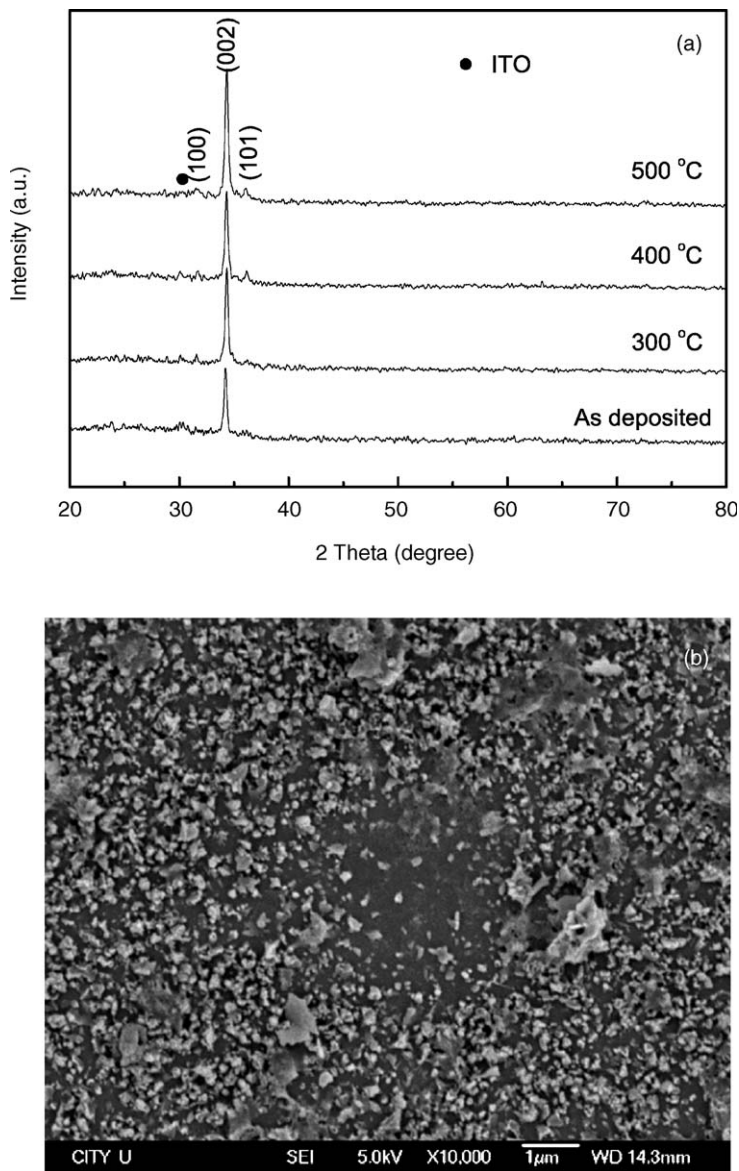


Fig. 1. (a) X-ray diffraction patterns of ZnO films prepared at room temperature and post-annealed at 300, 400, and 500 °C in air for 30 min. (b) The surface morphology of our ZnO thin film on ITO-coated glass substrate measured by SEM.

at 300 °C for 30 min in air is due to diffusion of oxygen and so the peak can be attributed to the  $[V_{O}^{\cdot+}]$  center.

With increasing annealing temperature or time, three visible emission bands at 432, 530, and 666 nm emerge and become more intense. Strong violet emission has recently been reported in oxygen-rich

ZnO films on silicon substrate at 6 K [17]. Using cathodeluminescence, Wu et al. found that a violet peak was induced by the zinc vacancy  $[V_{Zn}^{\cdot-}]$  center in stoichiometric ZnO films [8]. Hence, the violet emission band at 432 nm can be assigned to the  $[V_{Zn}^{\cdot-}]$  center, because the peak intensity increases with increasing annealing temperature in air ambient

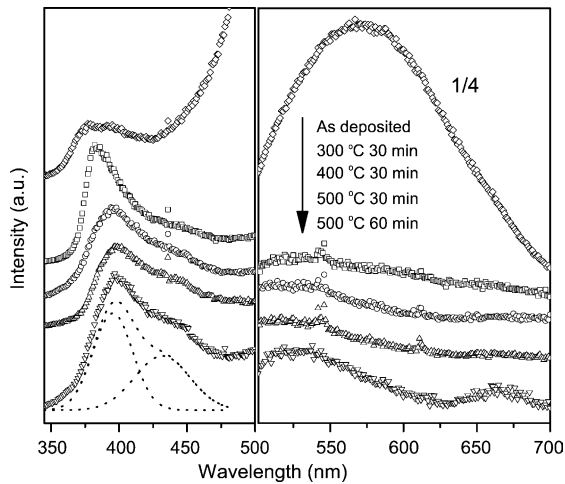


Fig. 2. Room-temperature PL spectra acquired from as-deposited and annealed ZnO films at different temperatures in air.

in which enough oxygen is supplied. There appears to be another mechanism for the weak green emission (530 nm) and the red emission (666 nm). In Shim's works, the diffusion of P atoms into the ZnO film is suggested to substitute P atoms for O atoms and generate interstitial oxygen [ $O_i^-$ ] centers that induce the emission at 640 nm [14]. This red band has also been observed in oxygen-rich ZnO films prepared by spray pyrolysis or pulsed laser deposition [8,18]. After annealing at 400 °C, another weak green band emerges in the oxygen-rich ZnO film, and it can be ascribed to the [ $O_i^-$ ] center. With increasing annealing temperature in air for our samples, the weak green emission (530 nm) and the red emission (666 nm) can be observed simultaneously. Therefore, we can deduce that the appearance and enhancement of these two bands arise from the increase of the interstitial oxygen [ $O_i^-$ ] center, and it agrees with the annealing effects on PL of ZnO films prepared by different methods [8,14].

Wurtzite ZnO belongs to the  $C_{6v}$  symmetry group, in which there exist Raman-active phonon modes  $E_2$  (low),  $E_2$  (high),  $A_1$  (TO),  $A_1$  (LO),  $E_1$  (TO), and  $E_1$  (LO), and the  $B_1$  modes are silent. Two obvious peaks (435 and 580  $\text{cm}^{-1}$ ) are observed in our ZnO films (Fig. 3). The former peak, whose intensity goes up with increasing annealing temperature, is the high frequency  $E_2$  of ZnO that has been previously identified [19]. On the other hand, the latter peak is quite controversial [20–22]. As we know, the four

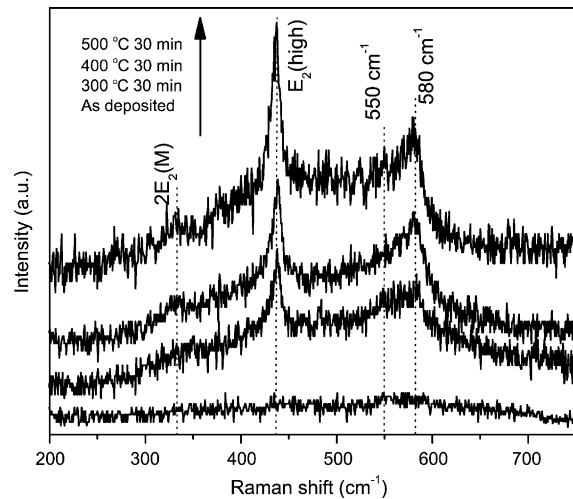


Fig. 3. Room-temperature Raman spectra obtained from as-deposited and post-annealed ZnO films at 300, 400, and 500 °C in air for 30 min.

possible mechanisms for the observed Raman scattering peaks near 580  $\text{cm}^{-1}$  involve the surface phonon mode,  $A_1$  (LO) mode,  $E_1$  (LO), and nitrogen-related local vibrational modes (LVMS) [20,21,23,24]. The surface phonon mode may disappear after annealing, while the intensity of the peak at 580  $\text{cm}^{-1}$  increases with increasing annealing temperature in our ZnO samples [23]. Therefore, this mode can be excluded. As for the  $A_1$  (LO) mode, it is not allowed in the backscattering configuration with crossed polarization adopted in our experiments [21,25]. The former two mechanisms should not be the cause of the Raman scattering peaks near 580  $\text{cm}^{-1}$ . Further investigation of Raman scattering near 580  $\text{cm}^{-1}$  in the ZnO film annealed in air at 300 °C reveals that there is a shoulder peak (550  $\text{cm}^{-1}$ ) near the main peak (580  $\text{cm}^{-1}$ ). A marked decrease in the intensity at 550  $\text{cm}^{-1}$  relative to that at 580  $\text{cm}^{-1}$  is observed with increasing annealing temperature, and the intensity of the 580  $\text{cm}^{-1}$  mode increases. With regard to the decrease of the  $E_1$  (LO) intensity reported by Exarhos and Sharma, two possible explanations have been suggested: thermal-induced crystallite reorientation and resonance enhancement of selective phonon modes due to lattice impurities [20]. No crystallite reorientation can be observed in our ZnO films by XRD. Another distinct feature of the  $E_1$  (LO) mode is that its

intensity decreases during annealing, and it is consistent with that of the  $550\text{ cm}^{-1}$  mode. It can thus be due to the  $E_1$  (LO) mode. On the contrary, the intensity of  $580\text{ cm}^{-1}$  mode increases during annealing. In Kaschner's work, it was found out that the intensity of N-related LVM increases with higher nitrogen concentration, and it agrees with the annealing behavior in air (N<sub>2</sub>) of our samples [21]. A theoretical calculation based on a modified valence-force model shows the value of  $272$  and  $580\text{ cm}^{-1}$  for LVMs of nitrogen on a substitutional oxygen site in the ZnO lattice [26]. Hence, the mechanism responsible for the  $580\text{ cm}^{-1}$  mode should be due to the N-related LVM. It is believed that the  $580\text{ cm}^{-1}$  mode and the shoulder peak mode ( $550\text{ cm}^{-1}$ ) originate from the N-related LVM and  $E_1$  (LO) mode, respectively, and it is helpful to distinguish the modes near the  $580\text{ cm}^{-1}$  peak.

#### 4. Conclusions

In conclusion, ZnO thin films with strong orientation (0 0 2) and smooth surface morphology were electrosynthesized on ITO-coated glass substrate at room temperature using pulsed voltage. PL shows an obvious violet band and strong green band. The former is due to the free-excitonic transition, and the latter is believed to stem from the single ionized oxygen vacancy ( $V_{\text{O}}^+$ ). Raman scattering reveals that the  $580\text{ cm}^{-1}$  peak and the shoulder peak ( $550\text{ cm}^{-1}$ ) originate from N-related LVMs and  $E_1$  (LO) mode, respectively.

#### Acknowledgements

One of the authors (Mei) thanks Mr. M.K. Tang and Dr. Amy X.Y. Lu for kind help in the experiments. This work was supported by the Grants (Nos. 10225416 and BK2002077) from the Natural Science Foundations of China and JiangSu province as well as Hong Kong Research Grants Council (RGC) Competitive Earmarked Research Grants (CERG) # CityU1052/02E and # CityU1137/03E.

#### References

- [1] B. Wacogne, M.P. Roe, T.A. Pattinson, C.N. Pannell, *Appl. Phys. Lett.* 67 (1995) 1674.
- [2] B. Ismail, M.A. Abaab, B. Rezig, *Thin Solid Films* 383 (2001) 92.
- [3] T. Mitsuya, S. Ono, K. Wase, *J. Appl. Phys.* 51 (1980) 2464.
- [4] T. Ikeda, J. Sato, Y. Hayashi, *Sol. Energy Mater. Sol. Cells* 34 (1994) 379.
- [5] J.S. Kim, H.A. Marzouk, P.J. Reocroft, C.E. Hamrin, *Thin Solid Films* 217 (1992) 133.
- [6] P. Bonasewicz, W. Hirschwald, G. Neumann, *Thin Solid Films* 142 (1986) 77.
- [7] J. Sang-Hun, B.-S. Kim, B.-T. Lee, *Appl. Phys. Lett.* 82 (2003) 2625.
- [8] X.L. Wu, G.G. Siu, C.L. Fu, H.C. Ong, *Appl. Phys. Lett.* 78 (2001) 2285.
- [9] A. Kuroyanagi, *Jpn. J. Appl. Phys.* 28 (1989) 219.
- [10] M.G. Ambia, M.N. Islam, M.O. Hakim, *J. Mater. Sci.* 29 (1994) 6575.
- [11] T. Pauporté, D. Lincot, *Electrochim. Acta* 45 (2000) 3345; M. Izaki, T. Omi, *Appl. Phys. Lett.* 68 (1996) 2439.
- [12] T. Mahalingam, V.S. John, P.J. Sebastian, *Mater. Res. Bull.* 38 (2003) 269.
- [13] Z.K. Tang, O.K.L. Wong, P. Yu, *Appl. Phys. Lett.* 72 (1998) 3270.
- [14] E.S. Shim, H.S. Kang, S.S. Pang, J.S. Kang, I. Yun, S.Y. Lee, *Mater. Sci. Eng. B* 102 (2003) 366.
- [15] S.-K. Kim, S.-Y. Jeong, C.-R. Cho, *Appl. Phys. Lett.* 82 (2003) 562.
- [16] K. Vanheusden, C.H. Seager, W.L. Warren, D.R. Tallant, J.A. Voigt, *Appl. Phys. Lett.* 68 (1996) 403.
- [17] S. Hun Jeong, B.-S. Kim, B.-T. Lee, *Appl. Phys. Lett.* 84 (2003) 2625.
- [18] S.A. Studenikin, N. Golego, M. Cocvera, *J. Appl. Phys.* 84 (1998) 2287.
- [19] J. Serrano, F.J. Manjón, A.H. Romero, F. Widulle, R. Lauck, M. Cardona, *J. Appl. Phys.* 84 (1998) 2287.
- [20] G.J. Exarhos, S.K. Sharma, *Thin Solid Films* 270 (1995) 27.
- [21] A. Kaschner, U. Habocek, M. Strassburg, M. Strassburg, G. Kaczmarczyk, A. Hoffmann, C. Thomsen, A. Zeuner, H.R. Alves, D.M. Hofmann, et al. *Appl. Phys. Lett.* 80 (2002) 1909.
- [22] C. Bundesmann, N. Ashkenov, M. Schubert, D. Spemann, T. Butz, E.M. Kaidashev, M. Lorenz, M. Grundmann, *Appl. Phys. Lett.* 83 (2003) 1974.
- [23] J. Xu, W. Ji, X.B. Wang, H. Shu, Z.X. Shen, S.H. Tang, *J. Raman Spectrosc.* 29 (1998) 613.
- [24] X. Wang, S. Yang, J. Wang, M. Li, X. Jiang, G. Du, X. Liu, R.P.H. Chang, *J. Cryst. Growth* 226 (2001) 123.
- [25] J.M. Calleja, M. Cardona, *Phys. Rev. B* 16 (1977) 3753.
- [26] G. Kaczmarczyk, A. Kaschner, A. Hoffmann, C. Thomsen, *Phys. Rev. B* 61 (2000) 5353.